

3-D traveltimes computation using a hybrid method

R. Coman and D. Gajewski¹

keywords: *traveltimes, wavefront construction, FD eikonal*

ABSTRACT

A hybrid method for computing multi-arrival traveltimes in 3-D weakly smoothed media is presented. The method is based on the computation of first-arrival traveltimes with a finite-difference eikonal solver (FDES) and the computation of later arrivals with the wavefront construction method (WFCM). The detection and bounding of regions where later arrivals occur is done automatically. WFCM is only used in complex models. If no triplications are present, only FDES is used. The complexity of the model is automatically investigated, without user intervention. The applicability of the method to a model with a triplication is demonstrated. The hybrid method is a better alternative to WFCM, since it is faster and has a comparable accuracy.

INTRODUCTION

Three-dimensional (3-D) traveltimes computation is commonly done with finite-difference eikonal solvers (FDESs) or with ray-tracing methods (e.g., Vidale, 1990; Cerveny, 1985). Only ray-tracing methods permit computation of multi-valued arrivals which occur in complex models, but for a prestack Kirchhoff migration this computation is very time consuming. Thus, a faster computation of 3-D multi-valued traveltimes is required.

FDESs provide a fast and robust method of first-arrival traveltimes computations (Vidale, 1990; van Trier and Symes, 1991; Sethian and Popovici, 1999). However, in complex velocity structures, first arrivals do not necessarily correspond to the most energetic wave, and other arrivals can also be important for accurate modeling and imaging (Geoltrain and Brac, 1993; Ettrich and Gajewski, 1996).

Multiple arrivals are traditionally computed with ray-tracing methods. The most suitable implementation of ray tracing for computing a large number of two-point problems is the wavefront construction method (WFCM) (Vinje et al., 1993; Ettrich

¹**email:** coman@dkrz.de

and Gajewski, 1996; Vinje et al., 1996; Lambaré et al., 1996). Unfortunately, the computational efficiency of WFCM is low (Leidenfrost et al., 1999).

Our aim is a more efficient computation of multi-valued 3-D traveltimes in weakly smoothed media. We combine FDES and WFCM to a hybrid method, taking advantages of the computational speed of FDES and using the ability of WFCM to compute multi-valued traveltimes. This idea was also used by Ettrich and Gajewski (1997) by presenting a related 2-D hybrid method. The corresponding 3-D hybrid method is not only an extension from 2-D, because many problems (e.g., the searching and bounding for regions where later transmitted arrivals occur) require new algorithms in 3-D.

The method that we present consists of four steps:

1. Computing of first-arrival traveltimes with a FDES,
2. Searching for triplications,
3. Bounding the regions where later arrivals occur,
4. Computing of later arrivals with WFCM.

After the computation of first-arrival traveltimes, the hybrid method will automatically realize if and where later arrivals occur. If no triplication is detected, computation with a fast FDES is sufficient. The implementation of the first and the last step is simple; the problems in developing a hybrid method are: the identification of zones where triplications occur, and the setting of initial conditions for WFCM.

We developed a new algorithm for the automatic detection and bounding of regions where later arrivals occur, and adapt a 3-D FDES (Vidale, 1990) and a 3-D WFCM (based on the implementation by Ettrich and Gajewski,1996) to the needs of the hybrid method.

THE FDES-WFCM HYBRID METHOD

We describe the four steps of the method by means of an example. The 3-D velocity model used in the example is a cube with a spherical inclusion in the middle (Figure 1). The $10 \times 10 \times 10$ km model used has a background velocity of 3.0 km/s. In the middle of the model is a spherical inclusion with a diameter of 3.5 km, where the velocity smoothly decreases to 1.5 km/s in the center of the inclusion. The source is located at coordinates $x = 5$ km, $y = 5$ km, $z = 0.5$ km. We choose this velocity distribution because it leads to a triplicated wavefront. The computed multi-valued wavefronts at three different traveltime steps are shown in Figure 2 . The bottom wavefront displays a triplication.

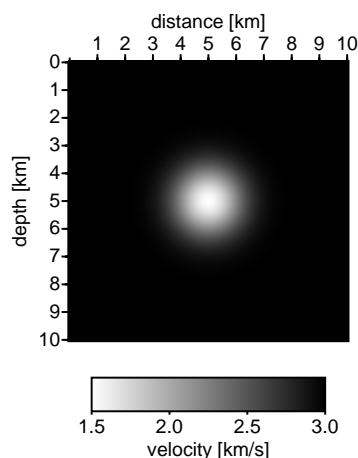


Figure 1: 2-D vertical slice through the middle of the 3-D velocity model. The 3-D velocity model used in the example is a cube with a spherical inclusion in the middle. The background velocity of 3.0 km/s smoothly decreases to 1.5 km/s in the middle of the inclusion.

The attributes of a triplication are important for understanding how the hybrid method works, so we define next two elements of a triplicated wavefront (see also Figure 3): (1) The wavefront crossing point is the point where two different wavefronts cross. The first-arrival wavefront shows in this point a discontinuity. (2) The reverse branch is the slowest branch of the triplication and it is formed by rays which already passed the caustic. This branch often carries the highest amount of energy. The reverse branch is the third arrival in a triplicated wavefront.

With help of the given definitions we explain the four steps of the hybrid method:

Step 1: Computing of first-arrival traveltimes with FDES

First-arrival traveltimes are computed with Vidale's FDES (Vidale, 1990), but we can also use other FDESs (van Trier and Symes, 1991; Sethian and Popovici, 1999). The first-arrival wavefronts, displayed in Figure 4, shows a region (at $x = 5 \text{ km}$ and $z > 6 \text{ km}$) where the traveltimes is not smooth. Discontinuous change of the wavefront curvature indicates wavefront crossing points, which we detect in the next step.

Step 2: Searching for triplications

For this step we use the first-arrival traveltimes computed in the step before. The searching for triplications in 3-D is more complicated than in 2-D, because the triplications can have complicated shape. Our algorithm is based on the fact that the traveltimes which belong to the same wavefront are smooth. We smooth the first-arrival traveltimes and subtract them from the original first-arrival traveltimes. The only differences will be near the wavefront crossing points (Figure

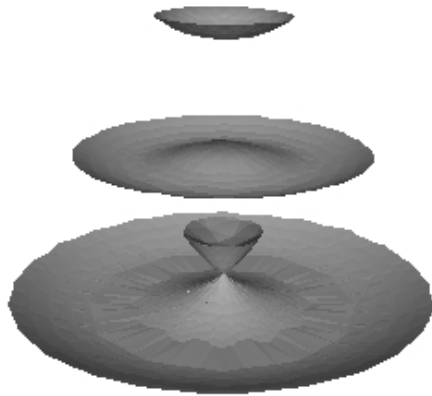


Figure 2: Wavefronts computed with WFCM for the model described above. The wavefronts are displayed at three different times (top 1 s, middle 2 s, bottom 3 s). The bottom wavefront shows a triPLICATION.

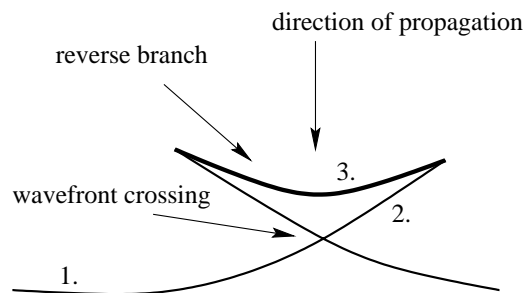


Figure 3: A triPLICATED wavefront. The reverse branch (bold; 3) of the triPLICATION is the slowest branch. The first and second arrivals belong to the same physical branch. They are separated by the wavefront crossing point.

5). At the end of this step we will have at the discretized subsurface model four points for each triPLICATION. The rays which connect the source point with these four points bound the region for the computation of later-arrival traveltimes with WFCM.

Step 3: Bounding the regions where later arrivals occur

Here, we find the rays which connect the source point with the four points fixed in the step before. So, we have to solve four two-point ray-tracing problems. The difficulty is that between each two points there are three different rays (see Figure 6). To solve this problem we developed a two-point ray-tracing method that works well in the vicinity of caustics and is robust, fast and accurate. Details about this method will be given in the next report. At the end of this step we will have the take-off angle for WFCM.

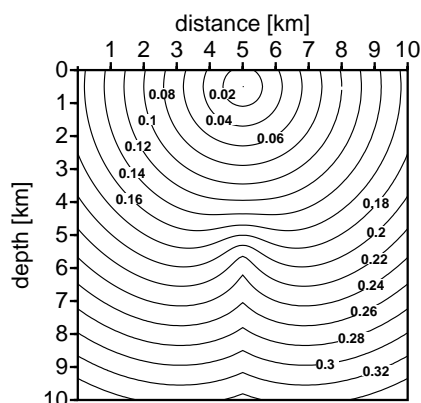


Figure 4: First-arrival traveltimes computed with Vidales's method. Regions at $x = 5 \text{ km}$ and $z > 6 \text{ km}$ displays wavefront crossing points. Note that this is a 2-D vertical slice of the 3-D traveltimes grid.

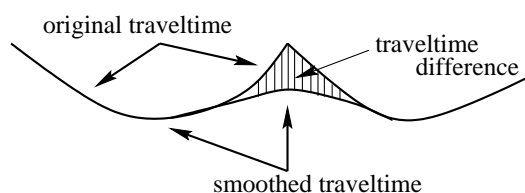


Figure 5: Searching for triplications. There are differences between original first-arrival traveltimes and the smoothed ones around the wavefront crossing points.

Step 4: Computing of later arrivals with WFCM

WFCM is performed only in the region delimitate by the four rays. Wavefronts built by rays which passed the caustic point are shown in Figure ???. 3-D WFCM is a relatively new approach to compute multi-valued traveltimes (Vinje et al., 1996). Based on the implementation of WFCM in 2-D media (Ettrich and Gajewski, 1996), we developed a 3-D WFCM and adapted it to the requirement of the hybrid method (the region is bounded by four rays and the interpolation to the traveltimes grid is done up to the first caustic point). We also tested new algorithms for the interpolation from wavefronts to the 3-D traveltimes grid and the interpolation of kinematic and dynamic ray-tracing parameters for a new ray. Also, several integration routines to perform ray tracing in the most efficient way were tested. Preliminary results show the Runge-Kutta method to be effective and accurate. Details about WFCM will be given in a following report.

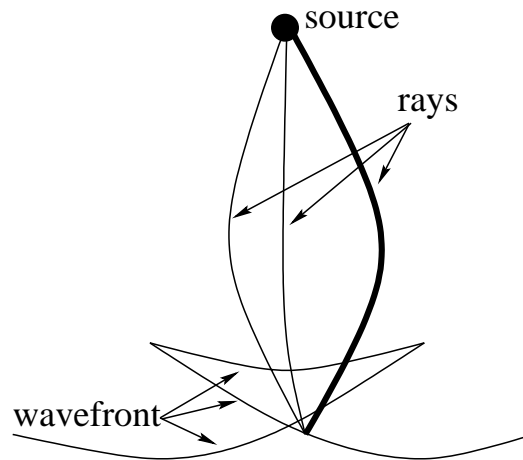


Figure 6: There are three rays between the source point and a point near the wavefront crossing point. We search only for the “first-arrival” ray (the bold one).

COMPUTATIONAL SPEED AND ACCURACY

Leidenfrost (1999) showed that for a 2-D model the computational speed with Vidale's FDES (Vidale, 1990) is higher than the one obtained with the WFCM method. Our tests show the same conclusion for a 3-D model. For the hybrid method we use this result and compute the first arrival with FDES, and only for the region where triplications occur, we compute later arrivals with WFCM. That leads to a faster code than with WFCM alone.

We compared the CPU-time between WFCM alone and the hybrid method for the 3-D velocity model (with $101 \times 101 \times 101$ gridpoints) described above. For a single shot, the computation with WFCM alone needs 75.1 s, while with the hybrid method only 38.41 s (Step 1. 17.45 s; Step 2. 1.02 s; Step 3. 0.9 s; Step 4. 19.04 s).

The computational speed of the hybrid method depends on:

1. The complexity of the model and the position of the source,
2. The accuracy of bounding the triplications,
3. The computational speed of each of the four steps discussed above.

The first point defines if the wavefront is single-valued or multi-valued. For a single-valued wavefront we compute the traveltimes only with FDES; for a multi-valued wavefront we additionally use the WFCM. The second point is important for models with triplications. If we bound each triplication accurately, we use WFCM for smaller regions, leading to a faster computation. The importance of the last point is obvious.

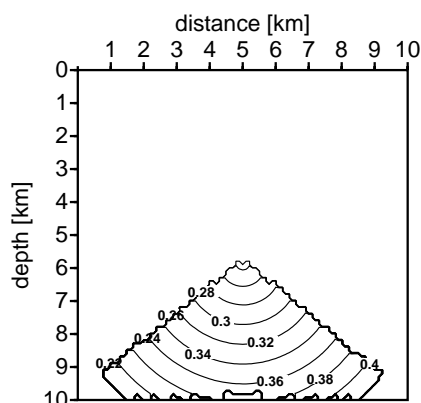


Figure 7: Wavefronts built by rays which passed the caustic. The later-arrival traveltimes are computed with WFCM.

The accuracy of traveltimes computed by the hybrid method is given by the accuracy of the applied FDES and by the ray-tracing parameters used in WFCM. Vidale (1990) analyzed his 3-D FDES and found a good accuracy. We found also a good accuracy for 3-D WFCM. This accuracy depends on: (1) the ray-tracing parameter, (2) the interpolation of ray-tracing parameter for a new ray, and (3) the traveltime interpolation from wavefronts to the 3-D traveltime grid of the discretized subsurface model.

CONCLUSIONS

The aim of this work was to develop a method for a more efficient computation of multi-valued 3-D traveltimes in weakly smoothed media. We propose a hybrid method that compute the first-arrival traveltimes with a fast FDES and use WFCM only in the region where later-arrivals occur.

The characteristics of our hybrid method are: (1) the computational *efficiency* is higher than for WFCM alone. We showed that for a single shot of the 3-D model we needed 75.1 s to compute the traveltimes with WFCM and only 38.41 s to compute them with the hybrid method; (2) the *accuracy* of traveltimes computed by the hybrid method is given by the accuracy of the applied FD eikonal solver and by the ray tracing parameters used in WFCM; (3) the decision if WFCM is needed is done *automatically*, i.e., no user intervention is necessary to decide the complexity of the model. Initial parameters for WFCM are also automatically determined.

ACKNOWLEDGEMENTS

This work was partially supported by the European Commission (JOF3-CT97-0029) and the sponsors of the WIT-consortium. Andree Leidenfrost made available his code for 3-D traveltimes computation (after Vidale, 1990). The initial computer code used for WFCM was developed by Norman Ettrich. We thank Ekkehart Tessmer, Boris Kastan, Tim Bergmann, Claudia Vanelle, Manfred Menyoli, and Tina Kaschwich for helpful discussion.

REFERENCES

- Cervený, V., 1985, The application of ray tracing to the numerical modeling of seismic wavefield in complex structure: *Handbook of Geophys. Expl.*, 15a, 1–124.
- Ettrich, N., and Gajewski, D., 1996, Wavefront construction in smooth media for pre-stack depth migration: *Pageoph*, **148**, 481–502.
- Ettrich, N., and Gajewski, D., 1997, A fast hybrid wavefront construction - FD eikonal solver method: 59th Mtg., Eur. Assoc. Expl Geophys., Extended Abstracts, E014.
- Geoltrain, S., and Brac, J., 1993, Can we image complex structures with first-arrival traveltimes?: *Geophysics*, **58**, 564–575.
- Lambaré, G., Lucio, P., and Hanyga, A., 1996, Two-dimensional multivalued travel-time and amplitude maps by uniform sampling of a ray field: *Geophys. J. Int.*, **125**, 584–598.
- Leidenfrost, A., Ettrich, N., Gajewski, D., and Kosloff, D., 1999, Comparison of six different methods for calculating traveltimes: *Geophys. Prosp.*, **47**, 269–297.
- Sethian, J. A., and Popovici, M. A., 1999, 3-D traveltimes computation using the fast marching method: *Geophysics*, **64**, 516–523.
- van Trier, J., and Symes, W. W., 1991, Upwind finite-difference calculation of traveltimes: *Geophysics*, **56**, 812–821.
- Vidale, J. E., 1990, Finite-difference calculation of traveltimes in three dimensions: *Geophysics*, **55**, 521–526.
- Vinje, V., Iversen, E., and Gjøystdal, H., 1993, Traveltime and amplitude estimation using wavefront construction: *Geophysics*, **58**, 1157–1166.
- Vinje, V., Iversen, E., Åstebøl, K., and Gjøystdal, H., 1996, Estimation of multivalued arrivals in 3D models using wavefront construction—part I: *Geophys. Prosp.*, **44**, 819–842.